Steady flow of viscoelastic fluids in microchannels under electrokinetic forces: PTT model with a Gordon–Schowalter convected derivative

S. Dhinakaran[1], A. M. Afonso[1] , M. A. Alves[1] and F. T. Pinho[2]

[1] CEFT, Departmento de Engenharia Química, Faculdade de Engenharia da Universidade do Porto,
Rua Dr. Roberto Frias, 4200 465 , Porto, Portugal
email: {dhina, aafonso, mmalves}@fe.up.pt http://www.fe.up.pt/~ceft
[2] Departmento de Engenharia Mecânica, Faculdade de Engenharia da Universidade do Porto,
Rua Dr. Roberto Frias, 4200 465 , Porto, Portugal
email: {fpinho}@fe.up.pt http://www.fe.up.pt/~ceft

Abstract

Analytical solutions for the electro-osmotic flow of viscoelastic fluids, in microchannels in the presence of electrokinetic forces, obeying the Phan-Thien-Tanner model have been derived. This model uses the Gordon–Schowalter convected derivative, which leads to non- zero second normal stress difference. The channel is assumed to be very long and flat so that the problem can be approximated to that of flow between two parallel plates. Symmetric boundary conditions with equal zeta potentials at the walls are assumed. A nonlinear Poisson–Boltzmann equation governing the electrical double-layer field and a body force caused by the applied electrical potential field are included in the Navier–Stokes equations. Results are presented for the velocity distribution between the parallel plates of the microchannel for different parametric values assumed that characterize this flow.

Keywords: Electro-osmotic flow, PTT viscoelastic fluid, Gordon–Schowalter derivative, analytical study

1 Introduction

The theoretical analysis of electro-osmotic flow of Newtonian fluids in microchannels has been the subject of several studies. Burgreen and Nakache [1] studied the effect of the surface potential on liquid transport through ultrafine capillary slits assuming the Debye–Hückel linear approximation to the electrical potential distribution under an imposed electrical field. Rice and Whitehead [2] discussed the same problem in a circular capillary. Dutta and Beskok [3] obtained analytical solutions for the velocity distribution, mass flow rate, pressure gradient, wall shear stress, and vorticity in mixed electro-osmotic / pressure driven flows for a two-dimensional straight channel geometry, for small, yet finite electrical double layer (EDL), relevant for applications where the distance between the two walls of a microfluidic device is about 1-3 orders of magnitude larger than the EDL thickness. Arulanandam and Li [4] presented a two-dimensional analytical model for the electro-osmotic flow in a rectangular microchannel.

The theoretical study of electro-osmotic flows of non-Newtonian fluids is recent and has been limited to simple inelastic fluid models, such as the power-law, due to the inherent analytical difficulties introduced by more complex constitutive equations. Examples are the recent works of Das and Chakraborty [5] and Chakraborty [6], who presented explicit relationships for velocity, temperature and concentration distributions in electro-osmotic microchannel flows of non-Newtonian bio-fluids described by the power-law model. Other purely viscous models were analytically investigated by Berli and Olivares [7], who considered the existence of a small wall layer depleted of additives and behaving as a Newtonian fluid (the skimming layer), under the combined action of pressure and electrical fields, thus restricting the non-Newtonian behavior to the electrically neutral region outside the electrical double layer. Very recently these studies were extended to viscoelastic fluids by Afonso et al [8], who presented analytical solutions for channel and pipe flows of viscoelastic fluids under the mixed influence of electro-kinetic and pressure forces, using two constitutive models: the PTT model (Phan - Thien and Tanner [9]), with linear kernel for the stress coefficient function and zero second normal stress difference [10], and the FENE-P model, based on the kinetic theory for Finitely Extensible Non-linear Elastic dumbbells with a Peterlin closure for the average spring force (cf. Bird et al [11]). Their analysis [8] was restricted to cases with small electric double-layers, where the distance between the walls of a microfluidic device is at least one order of magnitude larger than the EDL, and the fluid had a uniform distribution across the channel.

When the viscoelastic flow is induced by a combination of both electric and pressure potentials, in addition to the contributions from these two isolated mechanisms there is an extra term in the velocity profile that simultaneously combines both forcings, which is absent for the Newtonian and power-law fluids where the superposition principle applies. This extra term can contribute significantly to the total flow rate, and appears only when the rheological constitutive equation is non-linear. Afonso et al [12] extended this study to the flow of viscoelastic fluids under asymmetric zeta potential forcing, whereas Sousa et al [13] considered the effect of a skimming layer for the PTT fluid

When the viscoelastic flow is induced by a combination of both electric and pressure potentials, in addition to the contributions from these two isolated mechanisms there is an extra term in the velocity profile that simultaneously combines both forcings, which is absent for the Newtonian fluids where the superposition principle applies. This extra term can contribute significantly to the total flow rate, and appears only when the rheological constitutive equation is non-linear.

2 Problem statement

The geometry under consideration is shown schematically in **Fig**. **1**, where a microchannel is formed between two parallel plates separated by a distance (height) *2H*. The length of the channel is L_0 while the width is assummed to much larger than the height, *H*, i.e., $w >> 2H$. The bottom plate is located at $y = -H$ while the top plate is located at $y = +H$. A potential is applied along the axis of the channel which provides the necessary driving force for the flow. Due to the symmetry of the geometry with respect to the channel axis, only one half of the channel ($0 \le y \le H$) is considered for the analysis.

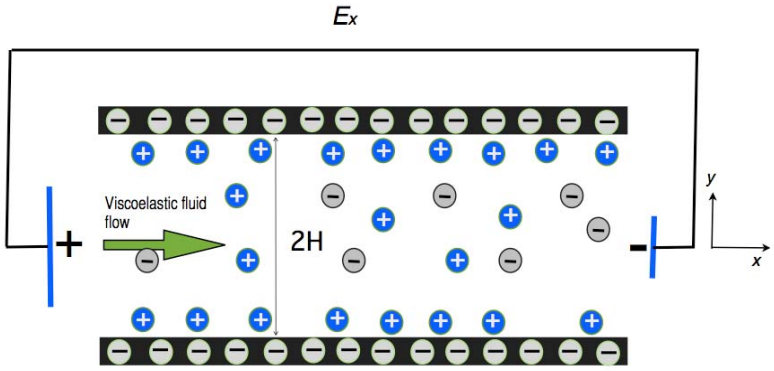

Fig. 1 Schematic of the microchannel geometry for the electro-osmotic flow of viscoelastic fluids considered in this study.

3 Governing equations

The equations governing the flow are the continutiy and the momentum equations

$$\nabla \cdot \rho \boldsymbol{u} = 0 \tag{1}$$

$$\frac{D\rho \mathbf{u}}{Dt} = -\nabla p + \nabla \cdot \boldsymbol{\tau} + \eta_s \nabla^2 u + \mathbf{F} \tag{2}$$

where $\boldsymbol{u}$ is the velocity vector, *t,* the time, ρ the fluid density, η_s is the Newtonian solvent viscosty and $\boldsymbol{\tau}$ the polymeric extra stress contribution. The $\boldsymbol{F}$ term in the modified momentum equatioins (2) represents the body force per unit volume, given by

$$\boldsymbol{F} = \rho_e \boldsymbol{E} \tag{3}$$

where $\boldsymbol{E}$ is the applied external electric field and ρ_e is the net electric charge density.

3.1 Constitutive equations

The model adopted here to describe viscoelastic behaviour is the PTT model (Phan-Thien and Tanner [9]), which can be expressed as

$$f\left(\tau_{kk}\right)\boldsymbol{\tau} + \lambda \overset{\diamond}{\boldsymbol{\tau}} = 2\eta \mathbf{D} \tag{4}$$

where **D** is the rate of deformation tensor, λ is a relaxation time, η is the polymer viscosity coefficient and τ represents the Gordon–Schowalter convected derivative usually defined as

$$\overset{\diamond}{\boldsymbol{\tau}} \equiv \frac{D\boldsymbol{\tau}}{Dt} - \nabla\mathbf{u}^T \cdot \boldsymbol{\tau} - \nabla\boldsymbol{\tau} \cdot \mathbf{u} + \xi\left(\boldsymbol{\tau} \cdot \mathbf{D} + \mathbf{D} \cdot \boldsymbol{\tau}\right) \tag{5}$$

where the parameter ξ accounts for the slip between the molecular network and the continuum medium. A simplified version of the above model is the so-called simplified Phan-Thien–Tanner (SPTT) equation where ξ = 0. The stress coefficient function, $f(\tau)$ is given by the linear form,

$$f\left(\tau_{kk}\right) = 1 + \frac{\varepsilon\lambda}{\eta}\tau_{kk} \tag{6}$$

where $\tau_{kk} = \tau_{xx} + \tau_{yy}$ represents the trace of the extra-stress tensor. When $f(\tau_{kk}) = 1$, the Johnson–Segalman (JS) constitutive equation, used for dilute polymer solutions, is recovered.

3.2 Poisson-Boltzmann equations

The equation for the potential field within the electric double layer (EDL), can be expressed by means of a Poisson-Boltzmann equation:

$$\nabla.\left(\nabla\psi\right) = -\frac{\rho_e}{\in} \tag{7}$$

where ψ denotes the EDL potential and $\in$ is the dielectric constant of the solution. The net electric charge density, ρ_e, can be described as

$$\rho_e = -2n_o ez \sinh\left(\frac{ez}{k_B T}\psi\right) \tag{8}$$

where, n_o is the ion density, e is the electronic charge and z is the ion valence.

3.3 Simplifying assumptions

To obtain a closed form analytical expression for the velocity distribution as a function of the viscoelastic parameters, the following simplifying assumptions are introduced:

1. The fluid is incompressible;
2. The velocity field is steady and fully developed, i.e., $u = u(y)$, $v = 0$;
3. The solvent viscosity is negligible, i.e., $\eta_s = 0$;
4. The Debye-Hückel linearization principle is valid. i.e., the EDL formed at the microchannel walls do not interfere with each other.
5. The flow is driven only by electrical effects (zero pressure gradient).

With these assumptions, the governing equations reduce to:

$$\nabla \cdot \mathbf{u} = \mathbf{0} \tag{9}$$

$$\nabla \cdot \boldsymbol{\tau} = -\rho_e \mathbf{E} \tag{10}$$

$$f\left(\tau_{kk}\right)\boldsymbol{\tau} + \lambda\overset{\diamond}{\boldsymbol{\tau}} = 2\eta\mathbf{D} \tag{11}$$

$$\nabla^2\psi = -\frac{\rho_e}{\in} \tag{12}$$

4 Analytical Solution

4.1 PTT consitutive equation

The predictions of the PTT model in this flow, for which $u = \{u(y),0,0\}$, can be obtained from equations (5) - (6), and leads to

$$f\left(\tau_{kk}\right)\tau_{xx} = \lambda(2-\xi)\dot{\gamma}\,\tau_{xy} \tag{13}$$

$$f(\tau_{kk})\tau_{yy} = \lambda\xi\dot{\gamma}\,\tau_{xy} \tag{14}$$

$$f(\tau_{kk})\tau_{xy} = \eta\dot{\gamma} + \lambda\left(1-\frac{\xi}{2}\right)\dot{\gamma}\,\tau_{yy} + \frac{\lambda\xi}{2}\dot{\gamma}\,\tau_{xx} \tag{15}$$

where $\tau_{kk} = \tau_{xx} + \tau_{yy}$ is the trace of the extra-stress tensor. Upon division of the expressions of equation (13) and (14) the specific function $f(\tau_{kk})$ and τ_{xy} cancels out, and a relation between two normal stresses is obtained,

$$\tau_{yy} = -\frac{\xi}{(2-\xi)}\tau_{xx} \tag{16}$$

leading to the following definition for the stress coefficient function:

$$f(\tau_{kk}) = 1 + \frac{2\varepsilon\lambda(1-\xi)}{\eta(2-\xi)}\tau_{xx} \tag{17}$$

Division of Eq. (15) by (13) results in a second order equation for the streamwise normal stress,

$$\lambda\xi\tau_{xx}^2 - \eta\tau_{xx} + \lambda(2-\xi)\tau_{xx} = 0 \tag{18}$$

which leads to the following physical solution for τ_{xx} (note that at the centerline, τ_{xx} and τ_{xy} should be zero)

$$\tau_{xx} = \frac{\eta}{2\lambda\xi}\left[1-\sqrt{1-\frac{4\lambda^2\xi(2-\xi)}{\eta^2}\tau_{xy}^2}\right] \tag{19}$$

4.2 Potential field within the electric double layer

The formation of the EDL in a fluid containing a small amount of charged species occurs when the presence of a charged surface on the microchannel walls causes a preferential redistribution of the charged species in the fluid. Then, in order to obtain the velocity field, first we need to solve the net charge density distribution (ρ_e). The charge density field can be calculated by combining equation (12), that under fully-developed flow conditions reduces to

$$\frac{d^2\psi}{dy^2} = -\frac{\rho_e}{\in} \tag{20}$$

and equation (8) to obtain the the well-known Poisson–Boltzmann equation,

$$\frac{d^2\psi}{dy^2} = -\frac{2n_o ez}{\in}\sinh\left(\frac{ez}{k_B T}\psi\right) \tag{21}$$

Primarily the electro-osmotic flow occurs with the migration of the charged species next to the microchannel walls subjected to an externally applied electric field. The migration of the charged species in the microchannel is governed by both the potential at the walls and by the externally applied electric field. For lower charge at the walls and small EDL thickness, this migration is mainly governed by the ζ potential at the wall. In this situation the charge distribution near the microchannel walls is affected very little by the external electric field ($\nearrow_0$), and can be determined independently. In fact, the effect of fluid motion on the charge redistribution can be neglected when the fluid velocity is small or the fluid is fully-developed, i.e., when the convective terms in the momentum equation are not dominant or when the EDL thickness is small. Then, for small values of ψ, the Debye–Hückel linearization principle ($\sinh x \approx x$) can be used, which means physically that the electrical potential is small compared with the thermal energy of the charged species, and the Poisson–Boltzmann equation can be transformed into the following linear form:

$$\frac{d^2\psi}{dy^2} = \kappa^2\psi \tag{22}$$

where, $\kappa^2 = 2n_0 ez / \in K_B T$ is the Debye–Hückel parameter, related with the thickness of the Debye layer, $\lambda_D =$

$1/\kappa$ (normally referred as the EDL thickness). This approximation is valid when the Debye thickness is small but finite, i.e., for $10 \leq H / \lambda_D \leq 10^3$.

Equation (22) can be solved subjected to the following boundary conditions: zeta potential at the wall, $\psi_{|y=H} = \psi_0$ and symmetry in the centerline, $(d\psi/dy)_{|y=0} = 0$,

$$\psi = \frac{\psi_0 \cosh(\bar{\kappa}\bar{y})}{\cosh(\bar{\kappa})} \tag{23}$$

which can be written in dimensionless form as:

$$\bar{\psi} = \frac{\cosh(\bar{\kappa}\bar{y})}{\cosh(\bar{\kappa})} \tag{24}$$

where $\bar{\psi} = \psi/\psi_0$, $\bar{\kappa} = \kappa H$ and $\bar{y} = y/H$.

Finally the net charge density distribution, equation (8), in conjunction with equations (23) reduces to

$$\rho_e = -\in \kappa^2 \frac{\psi_0 \cosh(\bar{\kappa}\bar{y})}{\cosh(\bar{\kappa})} \tag{25}$$

4.3 Analytical solutions for the PTT model

From the previous simplifications, the momentum equation (2), reduces to

$$\frac{d\tau_{xy}}{dy} = -\rho_e E_x \tag{26}$$

where $E_x \equiv d\varphi/dx$ and φ is the applied external electric potential.

Using equation (25) and noting that $\tau_{xy|y=0} = 0$ (centerline symmetry condition), Eq. (26) can be integrated to yield

$$\tau_{xy} = \in \psi_0 E_x \kappa \frac{\sinh(\kappa y)}{\cosh(\kappa H)} \tag{27}$$

Using the relation between the normal stress and shear stress - equation (19), an explicit expression for the normal stress component is obtained,

$$\tau_{xx} = \frac{\eta}{2\lambda\xi}\left[1 - \sqrt{1 - \frac{4\lambda^2\xi(2-\xi)}{\eta^2}\left(\frac{\in \psi_0 E_x \kappa}{\cosh(\kappa H)}\right)^2 \sinh^2(\kappa y)}\right] \tag{28}$$

The required boundary condition at the centerline, $\tau_{xy|y=0} = 0$, is consistent with equation (28). After combining (15), (27) and (28) we arrive to the important conclusion that the velocity gradient is given by

$$\dot{\gamma} = \frac{du}{dy} = \frac{\left[1 + \frac{2\varepsilon\lambda}{\eta}\frac{(1-\xi)}{(2-\xi)} \times \frac{\eta}{2\lambda\xi}\left\{1 - \sqrt{1 - \frac{4\lambda^2\xi(2-\xi)}{\eta^2}\left(\frac{\in \psi_0 E_x \kappa}{\cosh(\kappa H)}\right)^2 \sinh^2(\kappa y)}\right\}\right] \frac{\in \psi_0 E_x \kappa}{\cosh(\kappa H)} \sinh(\kappa y)}{\eta - \frac{\eta}{2}\left\{1 - \sqrt{1 - \frac{4\lambda^2\xi(2-\xi)}{\eta^2}\left(\frac{\in \psi_0 E_x \kappa}{\cosh(\kappa H)}\right)^2 \sinh^2(\kappa y)}\right\}} \tag{29}$$

Integrating eqn. (29) and applying the boundary condition ($u = 0$, at $y = H$) we obtain the velocity profile:

$$u = \frac{2\cosh(\kappa H)\left[\xi(2-\xi) + 2\varepsilon(1-\xi)\right]}{\left[4\lambda\kappa\xi(2-\xi)\right]\left(\frac{-\in \psi_0 E_x}{\eta}\right)} \times \left[\frac{1}{2}\ln\left(\frac{(1+B)(1-A)}{(1-B)(1+A)}\right) - \ln\left\{\frac{\tanh\left(\frac{\kappa y}{2}\right)}{\tanh\left(\frac{\kappa H}{2}\right)}\right\}\right]$$

$$-\frac{\varepsilon\xi(1-\xi)(2-\xi)\left(\frac{4\lambda\kappa}{\cosh(\kappa H)}\right)^2\left(\frac{-\in\psi_0 E_x}{\eta}\right)^2}{\left[\xi(2-\xi)+2\varepsilon(1-\xi)\right]}\left\{\cosh(\kappa H)-\cosh(\kappa y)\right\}$$

$$-\sqrt{4\lambda^2\xi(2-\xi)\kappa^2\left(\frac{-\in\psi_0 E_x}{\eta^2}\right)^2\left(\frac{1}{\cosh^2(\kappa H)}\right)}\left[\arcsin\left\{C\cosh(\kappa y)\right\}-\arcsin\left\{C\cosh(\kappa H)\right\}\right]\Bigg] \quad (30)$$

where,

$$A=\frac{\sqrt{2}\cosh(\kappa y)}{\sqrt{2+\frac{4\lambda^2\xi(2-\xi)\kappa^2}{\cosh(\kappa y)^2}\left(\frac{-\in\psi_0 E_x}{\eta}\right)^2-\frac{4\lambda^2\xi(2-\xi)\kappa^2}{\cosh(\kappa y)^2}\left(\frac{-\in\psi_0 E_x}{\eta}\right)^2\cosh(2\kappa y)}};$$

$$B=\frac{\sqrt{2}\cosh(\kappa H)}{\sqrt{2+\frac{4\lambda^2\xi(2-\xi)\kappa^2}{\cosh(\kappa H)^2}\left(\frac{-\in\psi_0 E_x}{\eta}\right)^2-\frac{4\lambda^2\xi(2-\xi)\kappa^2}{\cosh(\kappa H)^2}\left(\frac{-\in\psi_0 E_x}{\eta}\right)^2\cosh(2\kappa H)}}; \quad C=\sqrt{\frac{\frac{4\lambda^2\xi(2-\xi)\kappa^2}{\cosh(\kappa H)^2}\left(\frac{-\in\psi_0 E_x}{\eta}\right)^2}{1+\frac{4\lambda^2\xi(2-\xi)\kappa^2}{\cosh(\kappa H)^2}\left(\frac{-\in\psi_0 E_x}{\eta}\right)^2}}$$

Normalizing Eq. (30) with $De_k=\lambda\kappa u_{sh}$; $u_{sh}=\left(\frac{-\in\psi_0 E_x}{\eta}\right)$, we obtain the normalized velocity profile as

$$\frac{u}{ush}=\frac{2\cosh(\bar{\kappa})\left[\xi(2-\xi)+2\varepsilon(1-\xi)\right]}{\left[4\xi(2-\xi)\right]^2 De_k^2}\times\left[\frac{1}{2}\ln\left(\frac{(1+B)(1-A)}{(1-B)(1+A)}\right)-\ln\left\{\frac{\tanh\left(\frac{\bar{\kappa}\bar{y}}{2}\right)}{\tanh\left(\frac{\bar{\kappa}}{2}\right)}\right\}\right.$$

$$-\frac{\varepsilon\xi(1-\xi)(2-\xi)\left(\frac{4}{\cosh(\bar{\kappa})}\right)^2 De_k^2}{\left[\xi(2-\xi)+2\varepsilon(1-\xi)\right]}\left\{\cosh(\bar{\kappa})-\cosh(\bar{\kappa}\bar{y})\right\}$$

$$\left.-\sqrt{4\xi(2-\xi)De_k^2\left(\frac{1}{\cosh^2(\bar{\kappa})}\right)}\left[\arcsin\left\{C\cosh(\bar{\kappa}\bar{y})\right\}-\arcsin\left\{C\cosh(\bar{\kappa})\right\}\right]\right] \quad (31)$$

with ,

$$A=\frac{\sqrt{2}\cosh(\bar{\kappa}\bar{y})}{\sqrt{2+\frac{4\xi(2-\xi)}{\cosh^2(\bar{\kappa}\bar{y})}De_k^2-\frac{4\xi(2-\xi)}{\cosh^2(\bar{\kappa}\bar{y})}De_k^2\cosh(2\bar{\kappa}\bar{y})}}; \quad B=\frac{\sqrt{2}\cosh(\bar{\kappa})}{\sqrt{2+\frac{4\xi(2-\xi)}{\cosh^2(\bar{\kappa})}De_k^2-\frac{4\xi(2-\xi)}{\cosh^2(\bar{\kappa})}De_k^2\cosh(2\bar{\kappa})}};$$

$$C=\sqrt{\frac{\frac{4\lambda\xi(2-\xi)}{\cosh^2(\bar{\kappa})}De_k^2}{1+\frac{4\xi(2-\xi)}{\cosh(\kappa H)^2}De_k^2}}$$

A physical solution for the transverse profile of shear rate, in Eq. (30), occurs only when

$$\frac{4\lambda^2\xi(2-\xi)}{\eta^2}\left(\frac{\in\psi_0 E_x\kappa}{\cosh(\kappa H)}\right)^2\sinh^2(\kappa y)\le 1$$

In other words,

$$\sinh(\kappa y)\le\frac{2\lambda\sqrt{\xi(2-\xi)}}{\eta}\left(\frac{\in\psi_0 E_x\kappa}{\cosh(\kappa H)}\right) \quad (32)$$

Substituting Eq. (32) in Eq. (29), we get the critical shear rate to be

$$\lambda \dot{\gamma}_c = \frac{\varepsilon(1-\xi)+\xi(2-\xi)}{\left[\xi(2-\xi)\right]^{3/2}} \tag{33}$$

This critical shear rate depends on both ε and ξ. Above the maximum shear rate given in Eq. (33), the governing equations for the flow between the parallel plates do not have a real solution.

Another equations for the critical shear rate involving the the electric gradient (Ex) can also be obtained by substituting (32) in Eq. (29), given by

$$\lambda \dot{\gamma}_c = 2\frac{\lambda \in \psi_0 E_x \kappa}{\eta}\tanh(\bar{\kappa})\frac{\varepsilon(1-\xi)+\xi(2-\xi)}{\left[\xi(2-\xi)\right]} \tag{34}$$

Equating Eq. (33) and (34), we get an useful relation for the maximum electric gradient that can be applied at the microchannel walls for a given value of ε and ξ expressed as .

$$E_{x,c} = \frac{1}{2}\frac{\eta}{\in \psi_0 \lambda \kappa}\frac{1}{\tanh(\bar{\kappa})}\frac{1}{\sqrt{\xi(2-\xi)}} \tag{35}$$

Beyond this critical value of $E_{x,c}$ the flow becomes unstable.

5 Results and Discussion

The general equations for the flow of viscoelastic fluids in microchannels under the influence of electro-osmotic force were derived in the previous section. The influence of electro-osmotic force and fluid rheology on the velocity profile has been identified in Eq. (30). A few limiting cases contained in the general solutions are: (a) Newtonian fluid under the sole influence of electrokinetic forces and (b) viscoelastic fluid with zero second normal stress difference, i.e., the simplified Phan-Thien–Tanner (SPTT) equation with $\xi = 0$. A Fortran code has been written to numerically compute the velocity profiles.

For a Newtonian fluid the relaxation time is zero and the Deborah number vanishes ($De_\kappa = (\lambda\kappa/u_{sh}) = 0$, $\xi = 0$ and $\varepsilon = 0$), the velocity profile is only a function of the wall distance and the relative microchannel ratio, $\bar{\kappa}$, a shown earlier by Burgreen and Nakache [1]. **Fig. 2** shows the effect of the relative microchannel ratio, $\bar{\kappa}$ (or

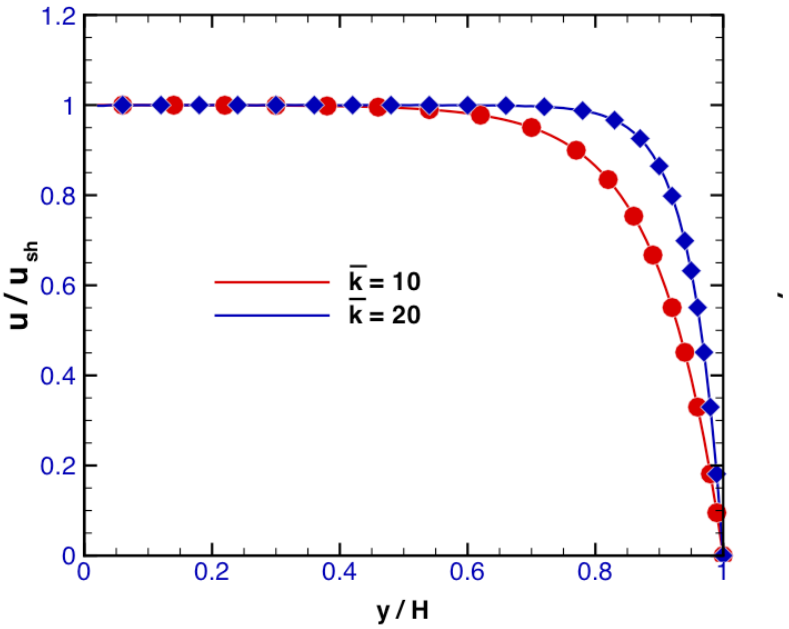

Fig. 2 Dimensionless velocity profiles for $\bar{\kappa}$ =10 and 20, for pure electro-osmosis Newtonian fluid flow. Symbols represent the data from Burgreen and Nakache [1].

H/λ_D, where λ_D is the Debye layer thickness) on the dimensionless velocity profiles (u/u_{sh}) for pure electro-osmotic flow. As $\bar{\kappa} \rightarrow 1$ the double layer thickness becomes of the same order of magnitude as the channel half-height and the region of excess charge is distributed over the entire channel. This situation is not fully compatible with this solution for which the Debye-Hückel approximation was invoked, which requires $\bar{\kappa} \geq 10$. For $\bar{\kappa} = 20$ the width of the Debye layer decreases, and the profile becomes more sharper near the wall.

The effect of De_k on the dimensionless velocity profiles is shown in **Fig. 3** at different Deborah numbers. At large Deborah number, the ratio u/ u_{sh} remains much greater than unity due to the shear-thinning nature of the viscosity of the PTT fluid and the lower viscosity at the wall region. With decrease in De_k, it decreases and at $De_k = 0.1$ and below, the dimensionless velocity profile remains unaltered.

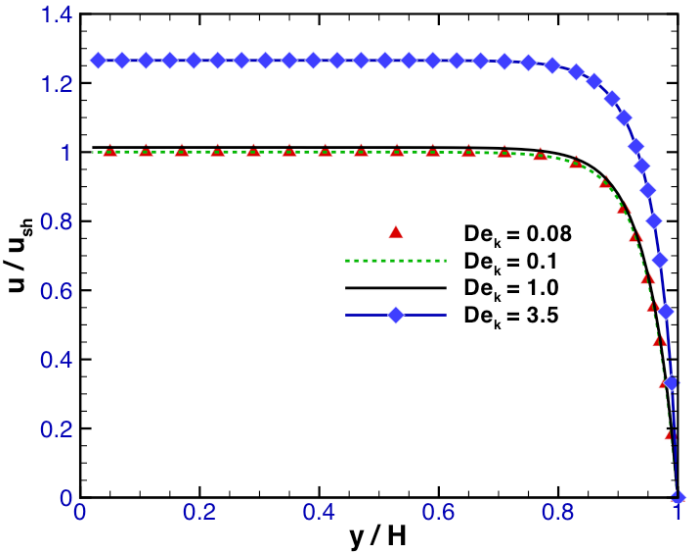

Fig. 3 Effect of De_k $(\varepsilon, \xi = 0.01)$ on the non-dimensional velocity profiles for the viscoelastic fluid flow between parallel plates under under the influence of electro-osmotic forces.

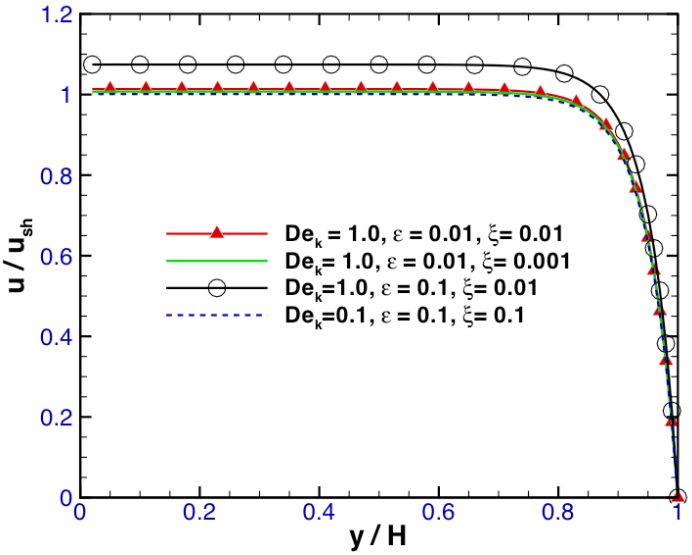

Fig. 4 Effect of ε and ξ on the non-dimensional velocity profiles for the viscoelastic fluid flow between parallel plates under the influence of electro-osmotic forces.

The flow between the parallel walls of the microchannel depends on various viscoelastic and electro-osmotic parameters. The influence of ε and ξ on the dimensionless transverse velocity profiles are plotted in **Fig. 4**. at

$De_k = 0.1$ and 1.0. For constant values of De_k and ε ($De_k = 1$ and $\varepsilon = 0.01$) for varying ξ, the dimensionless velocities at the center remain slightly greater than 1. Increasing ξ from 0.001 to 0.01, while maintaining a constant value of ($De_k\varepsilon$), we find that a decrease in velocity at $\xi = 0.001$ compared to the case when $\xi = 0.01$. At $De_k = 0.1$, the velocity profile approaches to the Newtonian solution even at $\varepsilon = 0.1$ and $\xi = 0.1$.

6 Conclusion

Analytical solutions for the electro-osmotic flow of viscoelastic fluids, in microchannels in the presence of electrokinetic forces, obeying the full PTT model have been derived. This model uses the Gordon–Schowalter convected derivative, which leads to non- zero second normal stress difference. Symmetric boundary conditions with equal zeta potentials at the walls are imposed. A nonlinear Poisson–Boltzmann equation governing the electrical double-layer field and a body force caused by the applied electrical potential field is included in the Navier–Stokes equations. The analytical solution was validated by comparing the results for a few limiting cases and was found to be in agreement with published results. Plots of non-dimensional, transverse velocity profiles elucidate the flow in the microchannel. The effect of Deborah number, ε and ξ on the velocity field has also been studied. Results are also presented for the critical values of shear rate and electric potential gradient beyond which flow instability occurs.

Acknowledgments

The authors are grateful to FCT for funding this work through grants number PTDC/EME-MFE/70186/2006 and PTDC/EQU-FTT/71800/2006. A. M. Afonso would also like to thank FCT for financial support through the scholarship SFRH/BD28828/2006.

References

1. D. Burgreen and F. R. Nakache, Electrokinetic flow in ultrafine capillary slits, *J. Phys. Chem.*, 68, 1084-1091, 1964.
2. C. L. Rice and R. Whitehead, Electrokinetic flow in a narrow cylindrical capillary. *J. Phys. Chem.*, 69, 4017–4024, 1965.
3. P. Dutta and A. Beskok, Analytical solution of combined electroosmotic / pressure driven flows in two-dimensional straight channels: finite Debye layer effects. *Anal. Chem.*, 73, 1979- 1986, 2001.
4. S. Arulanandam and D. Li, Liquid transport in rectangular microchannels by electro-osmotic pumping. *Colloids Surf. A.*, 161, 29–102, 2000.
5. S. Das and S. Chakraborty, Analytical solutions for velocity, temperature and concentration distribution in electroosmotic microchannel flows in a non- Newtonian bio-fluid. *Anal. Chim. Acta*, 559, 15-24, 2006.
6. S. Chakraborty, Electroosmotically driven capillary transport of typical non-Newtonian biofluids in rectangular microchannels, *Anal. Chim. Acta*, 605, 175-184, 2007.
7. M. L. Olivares, L. Vera- Candiotti and C. L. A. Berli, The EOF of polymer solutions, *Electrophoresis*, 30, 921-929, 2009.
8. A. M. Afonso, M. A: Alves and F. T. Pinho, Analytical solution of mixed electro-osmotic/ pressure driven viscoelastic fluids in microchannels, *J. Non-Newt. Fluid Mech.*, in press, 2009, doi:10.1016/j.jnnfm.2009.01.006
9. N. Phan-Thien and R. I. Tanner, New constitutive equation derived from network theory, *J. Non-Newt. Fluid Mech.* 2, 353–365, 1977.
10. N. Phan-Thien, ``A non-linear network viscoelastic model". *J. Rheo.*, 22, 259, 1978.
11. R. B. Bird, P. J. Dotson, N. L. Johnson, ``Polymer solution rheology based on a finitely extensible bead-spring chain model". J. Non-Newtonian Fluid Mech., 7, 213-235, 1980.
12. A. M. Afonso, M. A. Alves and F. T. Pinho, ``Electro-osmotic flows of viscoelastic fluids in microchannels under asymmetric zeta potential", in preparation, 2009.